Contents lists available at ScienceDirect

Science of the Total Environment

The role of afforestation species as a driver of Hg accumulation in organic horizons of forest soils from a Mediterranean mountain area in SW Europe

M. Méndez-López [a,b,*], A. Gómez-Armesto [a,b], F. Alonso-Vega [a,b], X. Pontevedra-Pombal [c], F. Fonseca [d], T. de Figueiredo [d], M. Arias-Estévez [a,b], J.C. Nóvoa-Muñoz [a,b]

[a] Universidade de Vigo, Departamento de Bioloxía Vexetal e Ciencia do Solo, Área de Edafoloxía e Química Agrícola, Facultade de Ciencias, As Lagoas s/n, 32004 Ourense, Spain
[b] Campus da Auga, Universidade de Vigo, Laboratorio de Tecnoloxía e Diagnose Ambiental, Rúa Canella da Costa da Vela 12, 32004 Ourense, Spain
[c] Departamento de Edafoloxía e Química Agrícola, Facultade de Bioloxía, Universidade de Santiago de Compostela, Rúa Lope Gómez de Marzoa s/n, 15786 Santiago de Compostela, Spain
[d] Centro de Investigação de Montanha (CIMO), Instituto Politécnico de Bragança, Campus de Sta Apolónia, 5300-253 Bragança, Portugal

HIGHLIGHTS

- Forest species influenced the Hg content and pool in soil organic horizons.
- Hg accumulation is strongly influenced by the organic matter decomposition degree.
- The uptake of atmospheric Hg by canopies influences its later accumulation in soils.
- Accumulated Hg can move to aquatic systems due to forest management and wildfires.
- Afforestation plans should select forest species considering environmental risks.

GRAPHICAL ABSTRACT
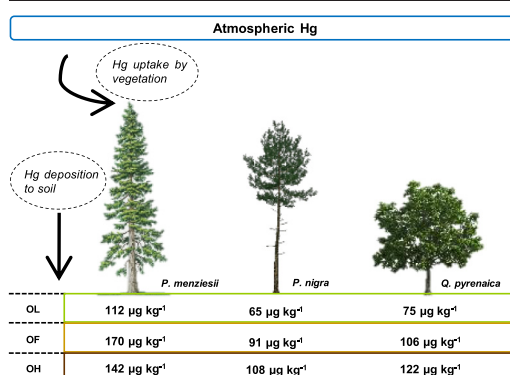
ARTICLE INFO

ABSTRACT

Forest areas are a primary sink of atmospheric mercury (Hg) within terrestrial ecosystems, whereas forest vegetation plays a key role in atmospheric Hg transfer to soil horizons. This study assessed variations in total Hg contents (Hg_T) and accumulation (Hg_{Res}) in the soil organic horizons of a forest area in NE Portugal, where post-wildfire afforestation led to the substitution of the native deciduous species (*Quercus pyrenaica*) by fast-growing coniferous species (*Pseudotsuga menziesii* and *Pinus nigra*). The study also evaluated, for each species, the links between Hg contents and other biophilic elements of soil organic matter (C, N, S) present in organic subhorizons (OL, OF, OH). Mean Hg_T in the organic horizons of the different tree species follow the sequence: *P. nigra* (88 µg kg^{-1}) < *Q. pyrenaica* (101 µg kg^{-1}) < *P. menziesii* (141 µg kg^{-1}). The highest Hg_{Res} for the entire organic horizon was found under *P. menziesii* (471 µg m^{-2}), followed by *P. nigra* (253 µg m^{-2}) and *Q. pyrenaica* (189 µg m^{-2}). Among the organic subhorizons, values of Hg_T and Hg_{Res} follow the sequence OL < OF < OH, which is consistent with the degree of organic matter humification. Indeed, Hg_T and Hg_{Res} correlated significantly with the C/N and C/S ratios for all species and organic subhorizons, suggesting that the quality of organic matter may influence strongly the Hg fate in these forest soils. Soils from *P. menziesii* plots have shown an Hg_{Res} 2.5 times higher than in plots dominated by the native *Q. pyrenaica*. Hg accumulation in the organic horizons, promoted in the coniferous species, may increase the risk of Hg mobilization due to wildfires and forest management practices. Therefore, forest management plans should select cautiously the tree species for afforestation in order to minimize adverse environmental effects caused by changes in the biogeochemical cycle of contaminants such as Hg.

* Corresponding author at: Universidade de Vigo, Departamento de Bioloxía Vexetal e Ciencia do Solo, Área de Edafoloxía e Química Agrícola, Facultade de Ciencias, As Lagoas s/n, 32004 Ourense, Spain.
  E-mail address: memendez@uvigo.es (M. Méndez-López).

1. Introduction

Terrestrial ecosystems are considered the major reservoir of Hg in the biosphere accumulating up to 1000 Gg of this global pollutant (Obrist et al., 2018). Although soils accumulate more than 90% of the Hg stored in terrestrial ecosystems (Engle et al., 2006; Obrist et al., 2009; Zhou et al., 2017), recent studies highlighted the key role of land cover vegetation (particularly forest species) in the biogeochemical cycle of Hg (Obrist et al., 2016; Wang et al., 2016a, 2019; Jiskra et al., 2018; Ma et al., 2019). In this sense, it is widely known that forest vegetation is actively involved in the removal of Hg from the atmosphere, either uptaking gaseous elemental Hg (Hg^0) through leave/needle stomata (Stamenkovic and Gustin, 2009; Rutter et al., 2011), or exerting a scavenging effect that favors the wet and dry deposition of oxidized Hg (Hg^{2+}) (Schroeder and Munthe, 1998).

Mercury accumulated in leaves/needles along their lifespan is transferred to soil surface through litterfall (Mosbaek et al., 1988). Indeed, litterfall has been shown as the main pathway for atmosphere-surface transfer of Hg in forest ecosystems (Zhou et al., 2013; Richardson and Friedland, 2015; Wang et al., 2016a; Navrátil et al., 2019; Gómez-Armesto et al., 2020a). After its deposition through litterfall, Hg is subjected to different biogeochemical reactions at the air-plant-soil interface that will determine the ultimate fate of Hg in forest ecosystems (Obrist et al., 2018; Ma et al., 2019). In this sense, there is a broad agreement on forest soils behaving as a net sink of long-term atmospheric Hg deposition which is closely related to soil organic C reservoirs (Smith-Downey et al., 2010; Obrist et al., 2011) as well as Al and Fe oxyhydroxides and metal (Al, Fe)-humus complexes (Guedron et al., 2009; Peña-Rodríguez et al., 2014; Navrátil et al., 2016; Gómez-Armesto et al., 2020b).

The amount of Hg stored in the forest floor is strongly influenced by litter biomass production (Wright et al., 2016). The production of litter biomass varies widely with the forest species resulting in higher fluxes of Hg deposition through litterfall in subtropical/tropical forests than in temperate/boreal ones (Wang et al., 2016a). Regarding temperate forests, fluxes of Hg deposited by litterfall also vary between coniferous and deciduous species (Obrist et al., 2012; Richardson and Friedland, 2015; Navrátil et al., 2016; Zhou et al., 2017). As a consequence, Hg reservoirs in the organic horizons of forest soils can differ depending on the dominant tree species (Obrist et al., 2012; Richardson and Friedland, 2015; Navrátil et al., 2016; Gruba et al., 2019). The degree of organic matter humification, which depends on the environmental conditions as well as the chemical composition of litterfall biomass, was also reported to influence Hg storage in the organic horizons (Obrist et al., 2009, 2011; Juillerat et al., 2012; Blackwell and Driscoll, 2015a). Therefore, the variation in the dominant tree species in forest ecosystems can change soil ability to store Hg and consequently, affect the biogeochemical Hg cycle at local, regional and global scales (Wang et al., 2019).

Presently, vegetation shift at a global scale, mainly driven by climate and land use changes (Gottfried et al., 2012), has been affecting directly and indirectly Hg occurrence and accumulation in the uppermost soil layers (Obrist et al., 2016; Jiskra et al., 2018). Thus, substitutions of tree species can arise from an adaptative response to new climatological conditions (Lindner et al., 2010), which could modify the amount of Hg transferred to the soil surface by litterfall (Richardson and Friedland, 2015; Obrist et al., 2016; Yang et al., 2019). Moreover, global warming can increase the mobilization of Hg stored in soil organic horizons through raising of the organic matter mineralization rate (Pokharel and Obrist, 2011; Blackwell et al., 2014) and/or through a higher frequency and severity of forest fires (Friedli et al., 2009; Webster et al., 2016; Kumar et al., 2018). Land use changes derived from the expansion of the agricultural frontier or due to different forestry practices have been also shown to disrupt soil Hg pools altering its biogeochemical cycle in terrestrial ecosystems (Almeida et al., 2005; Carpi et al., 2014; Mitchell et al., 2012; Eckley et al., 2018; Willacker et al., 2019).

Terrestrial ecosystems of the Mediterranean basin, considered highly sensitive to global warming (Guiot and Cramer, 2016), are exposed to a progressive agricultural land abandonment due to socio-economic factors (Terres et al., 2015) as well as to an increase in the occurrence and severity of forest fires (Versini et al., 2013). Both factors make large areas of the Iberian Peninsula highly vulnerable to soil loss by erosion and, to mitigate it, forest management practices substituting native species by non-native fast-growing ones were performed in the last decades. Consequently, significant changes in the stocks of C, N and S have been reported in the forest biomass and soil organic horizons (López-Marcos et al., 2018; Fonseca et al., 2019) and those of Hg are expected to occur.

In summary, the storage of Hg in forest soils is strongly influenced by the tree species in terms of litterfall fluxes, the organic matter decomposition rates in the forest floor and land use changes such as afforestation and forest fires (Gruba et al., 2019; Ma et al., 2019). Therefore, in the general context of Hg fate in terrestrial ecosystems, the main objective of this study is to assess potential changes in the concentration and reservoirs of Hg in the organic horizons of forest soils as a result of an afforestation process where a native deciduous species (*Quercus pyrenaica*) was replaced by coniferous species (*Pseudotsuga menziesii* and *Pinus nigra*). In addition, the influence of proxies of organic matter decomposition (C/N and C/S ratios) and ratios of biophilic elements (C, N and S) to Hg (Hg/C, Hg/N and Hg/S), are assessed depending on the tree species and type of organic subhorizon. Results of the research conducted are interpreted in terms of Hg mobilization risks (leaching, loss in runoff, re-volatilization) that would arise from forest management or forest fires.

2. Material and methods

2.1. Study area and soil sampling

The study area is located in Serra da Nogueira (NE Portugal), a mid-altitude mountain range with summits about 1300 m a.s.l. The climate in the area is Mediterranean with a slight Atlantic influence (mean annual temperature of 12 °C and total annual precipitation of 1100 mm). The native forest vegetation is dominated by the deciduous species *Quercus pyrenaica* (QP), but due to recurrent forest fires in the area, afforestation was conducted several decades ago introducing fast-growing coniferous species such as *Pseudotsuga menziesii* (PM) and *Pinus nigra* (PN). The lithology in the area is dominated by metamorphic rocks, mainly schists and some slates, thus most of the forest soils can be classified as Umbrisols and Leptosols (IUSS Working Group WRB, 2015).

In the study area, three different stands dominated by old-growth native QP and 30-year-old plantations of PM and PN were selected for soil sampling purposes. The stands are less than 2 km far from each other and all of them have similar characteristics in terms of altitude, soil parental material, topography and climatic conditions. Additional information about the forestry characteristics of the stands is reported by Fonseca et al. (2019). In each stand, three circular plots of 314 m^2 were established and five square subplots of 0.5 m^2 (70 × 70 cm) were distributed randomly within the circular area ensuring they were 50 m away of any forest path.

In the 45 square subplots (15 per tree species), all the mass of the organic horizons present in each square subplot was separated in the following subhorizons according to the occurrence of the recognizable organic matter remains: OL (organic layer with undecomposed and distinguishable surface litter), OF (organic layer with partially decomposed litter) and OH (organic layer with decomposed and indistinguishable litter in the form of humus), according to Zanella et al. (2018).

During soil sampling, nitrile free-powder gloves, a plastic garden trowel and a small saw were used to collect the samples and for their transference to polyethylene bags, which were kept at 4 °C in a portable fridge before transporting them to the laboratory. Between samples collection, gloves and sampling material were rinsed with double-distilled water to prevent potential cross-contamination. The average thickness of each organic subhorizon was estimated from values recorded in the field at the corners of the square subplots ($n = 4$).

2.2. Soil sample preparation and chemical characterization

Soil samples corresponding to OL, OF and OH subhorizons were air-dried at 40 °C for one week. After the removal of living understory vegetation (herbs, grasses, mosses, lichens), as well as twigs, branches and bark pieces above 2 cm in length, cones and acorns, samples ($n = 135$) were weighted to estimate mass per unit area. Afterwards, soil samples were ground until reaching a particle size <4 mm using a cutting mill (Retsch SM 100) and homogenized. A small fraction of the ground samples (5 g) was finely milled in an agate mortar (Retsch RM 200) to reduce the particle size up to <50 μm and increase sample homogeneity.

Soil pH was measured in distilled water (pH_w) and 0.1 M KCl (pH_k) using a 2:5 soil/solution ratio after contact times of 10 min and 2 h, respectively. Effective cation exchange capacity (eCEC) was estimated as the sum of base cations (Ca, Mg, Na and K) displaced with 1 M NH$_4$Cl (Sumner and Miller, 1996), and assuming negligible amounts of exchangeable Al in the organic horizons. Base cations were determined by flame atomic absorption (or emission) spectroscopy with a Thermo-Elemental Solaar spectrometer. Both, soil pH and eCEC were performed on ground samples (<4 mm). Total contents of organic C, N and S were determined in finely milled samples using a combustion analyzer (LECO CNS 2000).

2.3. Total mercury determination

Total Hg (Hg_T) was determined in, approximately, 100 mg of finely milled soil samples using a Milestone DMA-80 Direct Mercury Analyzer. The basis of the method used is thermal decomposition, Au-amalgamation and atomic absorption spectrophotometry (U.S. EPA, method 7473). All samples were analyzed in duplicates and when replicates deviated more than 10%, the analysis was repeated until obtaining a satisfactory replication. The limit of detection (LOD) was 0.43 μg kg^{-1} (calculated as 3 times the standard deviation of 10 blank measurements). For quality assurance and quality control (QA/QC), standard reference materials NIST 1547 (peach leaves, 31 ± 7 μg kg^{-1}), BCR 142R (soil, 67 ± 11 μg kg^{-1}) and NCS ZC 73018 (citrus leaves, 150 ± 20 μg kg^{-1}) were measured at the beginning of the analysis and after every twelve measurements. The percentages of recovery were 99, 103 and 108%, respectively. All Hg_T values are expressed as the oven-dry weight (105 °C).

The reservoir or pool of Hg in each organic subhorizon (Hg_{Res}), i.e. the amount of Hg stored in soil in terms of area, expressed as μg m^{-2}, was calculated as shown in Eq. (1), according to Zhou et al. (2017),

$$Hg_{Res} = Hg_T \times q_{am} \qquad (1)$$

where Hg_T is the total Hg concentration in each OL, OF and OH subhorizon expressed in μg kg^{-1}, respectively. q_{am} is the dry mass of each organic subhorizon sampled in a square plot (70 × 70 cm), expressed as kg m^{-2}.

The amount of Hg stored in the entire organic horizon (Hg_{ResT}) is calculated as the sum of the individual Hg reservoirs obtained for each organic subhorizon. The C, N and S reservoirs (pools) of the organic subhorizons (C_{Res}, N_{Res} and S_{Res}) were calculated using the same procedure.

2.4. Statistical analyses

Statistical analyses, using non-parametric statistics, were carried out by IBM SPSS Statistics 25 software for Windows. The relevance of statistical correlations was evaluated by means of the Spearman rank test (rho) whereas the Kruskal-Wallis test was used to assess the type of organic subhorizon and the forest species as influencing factors for Hg_T, Hg_{Res} and soil chemical characteristics. Moreover, Mann Whitney and Wilcoxon tests were performed pairwise by tree species or organic subhorizons trying to find out significant differences between them. For all statistical tests, significance was considered when $p < 0.05$ unless otherwise noted. Finally, descriptive analyses were done to obtain average and standard deviations for all measured and calculated parameters.

3. Results

3.1. General chemical characterization of the organic horizons

Mean values of soil pH in distilled water (pH_w) ranged from 4.7 to 6.0 showing an increase from the OL to the OH subhorizons regardless the dominant species (Table 1). pH measured in saline solution (pH_k), slightly more acid (range 4.2–5.6), showed a similar trend than pH_w. Total organic C content presented a wide range of mean values (200–533 g kg^{-1}; Table 1), with the highest ones in the OF horizons from *P. nigra* plots. In contrast, maximum averages of total N (range 7.4–15.9 g kg^{-1}) and total S (range 0.8–1.5 g kg^{-1}) occurred in the samples collected from *Q. pyrenaica* plots. The C/N and C/S ratios, both expressed as g/g, showed mean values from 24 to 58 and from 244 to 538, respectively. For both ratios, mean values decreased from the OL to the OH subhorizons for each species (Table 1). Significant differences (Kruskal-Wallis test, ($p < 0.05$) in the above-mentioned soil parameters were found between tree species and type of organic subhorizons (Tables S1 and S2, respectively). The average of the sum of exchangeable base cations (SB, Table 2) ranged from 22 to 50 cmol$_c$ kg^{-1}, with the lowest values in the samples from *P. nigra* plots and the highest in those collected from *P. menziesii* plots. Among the base cations, exchangeable Ca (Ca_e) was by far the dominant cation occupying more than 64% of the available sites in the cation exchange complex of all organic horizons. The abundance of other exchangeable base cations decreased according to the sequence: Mg ≫ K > Na (Table 2). Mostly, exchangeable contents of Ca, Mg and K differed significantly depending on the dominant tree species in the plot as well as the type of organic subhorizon (Tables S1 and S2).

3.2. Total Hg in the organic horizons: concentrations and pools

The mean value of total Hg concentration (Hg_T) in the organic subhorizons was 110 μg kg^{-1} (range 50–214 μg kg^{-1}; $n = 134$). As the Hg_T in the organic horizons differed significantly depending on the dominant forest species in the plot after application of a Kruskal-Wallis test (H = 54.045; $p = 0.000$; n = 134), their values have been described separately. In the plots dominated by the native species (*Q. pyrenaica*), the average Hg_T ranged from 75 μg kg^{-1} in the OL subhorizon to 122 μg kg^{-1} in the OH subhorizon (Fig. 1). Regarding the afforested species,

Table 1
Mean values and standard deviation of selected properties of the organic subhorizons in the studied plots ($n = 15$).

| Tree species	Hor	Thickness	Areal dry mass	pH_w	pH_k	C	N	S	C/N	C/S
		cm	g m^{-2}				g kg^{-1}			
Q. pyrenaica	OL	6.6 ± 0.9	586 ± 108	5.0 ± 0.2	4.6 ± 0.1	450 ± 5	14.7 ± 1.0	1.5 ± 0.1	31 ± 2	311 ± 21
	OF	3.6 ± 0.5	377 ± 130	5.3 ± 0.2	5.0 ± 0.2	476 ± 40	15.9 ± 1.0	1.5 ± 0.1	30 ± 3	311 ± 31
	OH	3.8 ± 0.8	832 ± 365	5.6 ± 0.2	5.1 ± 0.2	345 ± 63	14.1 ± 1.6	1.4 ± 0.2	24 ± 2	244 ± 27
P. menziesii	OL	1.7 ± 0.3	720 ± 333	5.3 ± 0.3	5.0 ± 0.3	458 ± 17	10.9 ± 1.0	1.1 ± 0.1	42 ± 4	405 ± 44
	OF	2.5 ± 0.9	946 ± 289	5.7 ± 0.3	5.5 ± 0.2	427 ± 47	12.1 ± 1.4	1.2 ± 0.1	35 ± 3	343 ± 27
	OH	2.2 ± 0.9	1607 ± 412	6.0 ± 0.3	5.6 ± 0.2	201 ± 46	7.4 ± 1.4	0.8 ± 0.2	27 ± 3	256 ± 21
P. nigra	OL	5.5 ± 0.8	695 ± 360	4.7 ± 0.2	4.2 ± 0.2	473 ± 14	8.4 ± 1.5	0.9 ± 0.2	58 ± 10	538 ± 100
	OF	4.0 ± 1.1	855 ± 601	4.8 ± 0.3	4.3 ± 0.3	533 ± 51	11.0 ± 1.8	1.1 ± 0.2	50 ± 10	478 ± 96
	OH	2.4 ± 0.6	1168 ± 557	5.0 ± 0.3	4.5 ± 0.3	380 ± 65	11.1 ± 2.3	1.2 ± 0.3	35 ± 7	334 ± 61

Table 2

Mean values and standard deviation of parameters of the cation exchange complex of the organic subhorizons in the studied plots.

Tree species	Hor	Na_e	K_e	Ca_e	Mg_e	SB^a
				$cmol_c\ kg^{-1}$		
Q. pyrenaica	OL	0.7 ± 0.7	2.9 ± 0.9	24.4 ± 8.8	9.0 ± 2.2	37.0 ± 9.8
	OF	0.5 ± 0.3	1.9 ± 0.4	29.4 ± 7.6	9.7 ± 1.7	41.5 ± 8.3
	OH	0.4 ± 0.2	1.2 ± 0.3	28.0 ± 8.5	8.2 ± 2.6	37.8 ± 9.0
P. menziesii	OL	0.5 ± 0.2	3.2 ± 0.8	25.5 ± 9.1	8.6 ± 1.2	37.9 ± 10.0
	OF	0.6 ± 0.4	2.2 ± 0.5	39.1 ± 11.3	7.8 ± 2.1	49.6 ± 12.1
	OH	0.4 ± 0.2	1.4 ± 0.5	28.9 ± 8.1	5.5 ± 2.2	36.1 ± 9.7
P. nigra	OL	0.5 ± 0.3	2.9 ± 0.5	15.4 ± 4.3	5.5 ± 1.5	24.2 ± 5.1
	OF	0.4 ± 0.3	2.6 ± 0.4	18.9 ± 5.3	4.9 ± 1.5	26.9 ± 5.9
	OH	0.5 ± 0.4	1.8 ± 0.4	16.2 ± 4.9	4.0 ± 0.8	22.5 ± 5.4

[a] SB: sum of exchangeable base cations.

mean values of Hg_T in samples from *P. nigra* plots (range 65 to 108 µg kg^{-1}) were relatively similar to those collected under the native species (Fig. 1), although there were significant differences for Hg_T in the OL subhorizons of the soils beneath *P. nigra* and *Q. pyrenaica* after a Wilcoxon test (Z = −2.045; p = 0.041). In the *P. menziesii* plots, the average of Hg_T ranged from 112 µg kg^{-1} in the OL subhorizons to 170 µg kg^{-1} in the OF subhorizons, being significantly higher than those found in *P. nigra* or *Q. pyrenaica* plots for all organic subhorizons.

Total Hg content in the samples collected under each tree species also differed significantly depending on the type of organic subhorizon (H = 39.553; p = 0.000; n = 134). In the plots dominated by *Q. pyrenaica* and *P. nigra*, Hg_T increased following the sequence OL < OF < OH (Fig. 1), but in the *P. menziesii* plots the peak of Hg_T occurred in the OF subhorizon (Fig. 1).
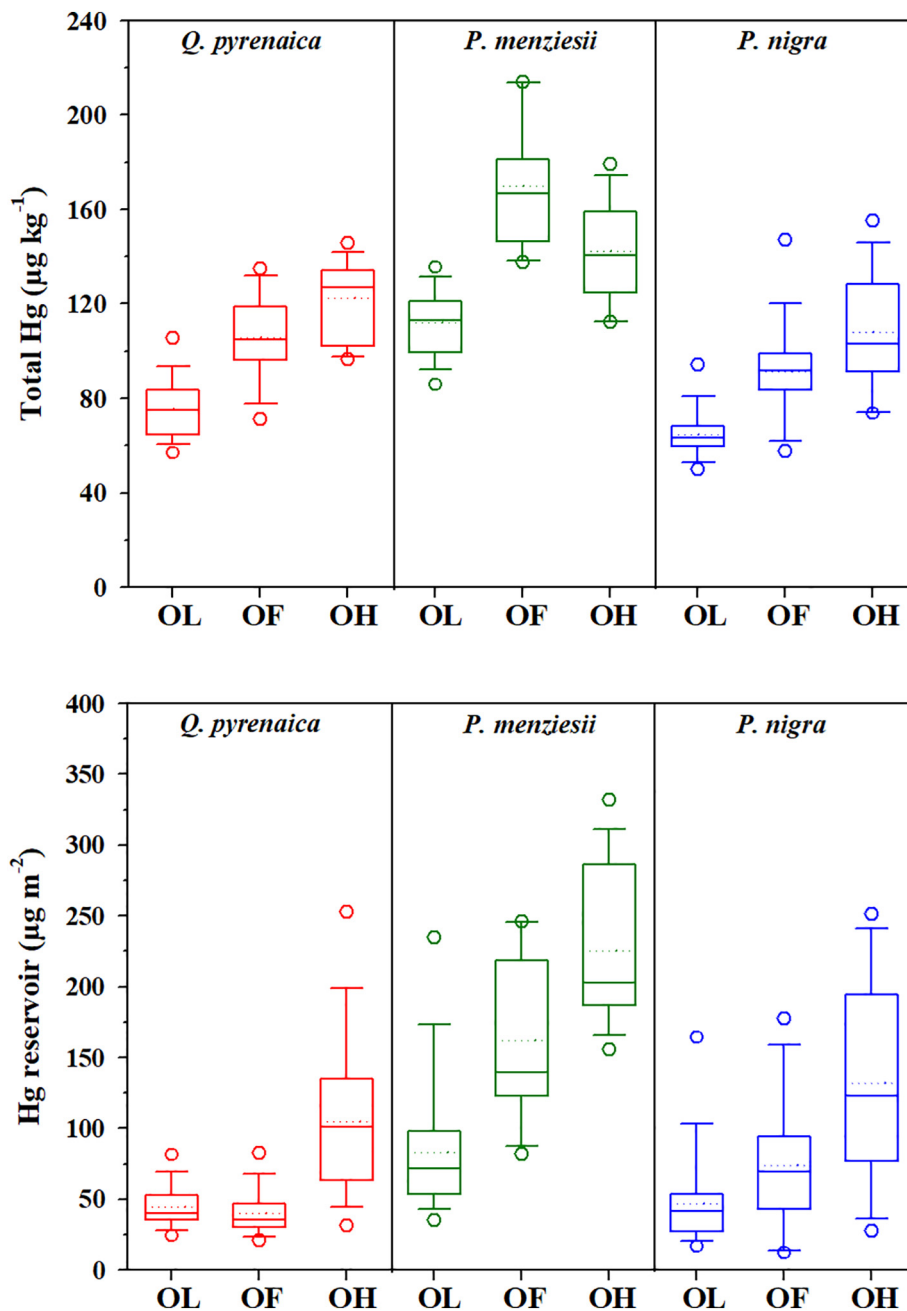
Fig. 1. Box and whisker plot of total Hg concentrations (top) and Hg reservoir (bottom) for each species and organic subhorizon. The box indicates the interquartile range (from 25 to 75 percentiles) whereas lines in the box mark the median (solid line) and the average (dashed line). Whiskers above and below the box indicate the 90th and 10th percentiles and outliers are represented by empty circles.

The mean amount of Hg stored in the organic subhorizons, i.e. Hg reservoir (Hg$_{Res}$), was 101 µg m^{-2} (range 12–332 µg m^{-2}) showing significant differences depending on the tree species (H = 37.985; p = 0.000; n = 134). In the plots covered by *Q. pyrenaica*, the mean values of Hg$_{Res}$ varied from 45 to 104 µg m^{-2} in the OL and OH subhorizons, respectively (Fig. 1). Somewhat higher values of Hg$_{Res}$ were found in samples from plots dominated by coniferous species (*P. menziesii* and *P. nigra*), particularly in the case of *P. menziesii*. The average of Hg$_{Res}$ in the plots of *P. menziesii* was 83 µg m^{-2} (OL), 162 µg m^{-2} (OF) and 226 µg m^{-2} (OH), whereas in those of *P. nigra* the averages were 47, 74 and 132 µg m^{-2} for the subhorizons OL, OF and OH, respectively (Fig. 1).

Taking into account the entire organic horizon (i.e., OL + OF + OH), the lowest Hg storage (Hg$_{ResT}$) was observed for the plots dominated by the native species (*Q. pyrenaica*) with an average of 189 µg m^{-2} (range 99–343 µg m^{-2}). The values of Hg$_{ResT}$ in QP plots did not differ significantly from those of *P. nigra* plots (mean 253 µg m^{-2}; range: 80–473 µg m^{-2}). However, the values of Hg$_{ResT}$ for the organic horizons of the *P. menziesii* plots was considerably higher than those for the other species, reaching a mean value of 471 µg m^{-2} (range 328–653 µg m^{-2}).

As in the case of Hg$_T$, the amount of Hg stored in the organic horizons (Hg$_{Res}$) was also significantly different when comparing organic subhorizons (H = 36.198; p = 0.000; n = 134) with a gradual increase following the sequence OL < OF < OH (Fig. 1). The OL and the OF subhorizons in QP plots did not follow this trend as their Hg storage was not significantly different (Wilcoxon test; Z = −1.335; p = 0.182).

3.3. Relationships between Hg and biophilic elements of soil organic matter

The relationships between Hg and major biophilic elements of soil organic matter (C, N and S) have been widely used to compare Hg contents and its storage in forest soils to overcome the effects of organic matter accumulation (Åkerblom et al., 2008; Obrist et al., 2009; Yu et al., 2014; Navrátil et al., 2014, 2016; Wang et al., 2016b). For this reason, the ratios Hg/C, Hg/N and Hg/S were also examined in the organic subhorizons of the plots studied.

The mean value of the Hg/C ratio of all samples was 0.3 µg Hg g^{-1}C (range 0.1–0.9 µg Hg g^{-1}C) and the tree species was found to be a factor that introduced significant variation in this ratio (H = 49.675; p = 0.000; n = 134). The average of the Hg/C ratio obtained for OL and OH subhorizons from *Q. pyrenaica* and *P. nigra* plots was quite similar, ranging from 0.17 to 0.36 and 0.14 to 0.29 µg Hg g^{-1}C, respectively (Fig. 2). In the samples from *P. menziesii* plots, the Hg/C ratio mean values were higher (range 0.25–0.73 µg Hg g^{-1}C), particularly in the OH subhorizons that duplicate those for the same subhorizon in the QP (0.36 µg Hg g^{-1}C) and PN

plots (0.29 µg Hg g^{-1}C) (Fig. 2). When the Hg/C ratio was examined for each species separately, the type of organic subhorizon arose as a significant factor of variance and in all cases the Hg/C ratio increased progressively following the sequence: OL < OF < OH. The Hg/C ratio in OH subhorizons was 3.0, 2.1 and 2.2 times higher than those of OL horizons in the plots dominated by PM, PN and QP, respectively.

The Hg/N ratio was also significantly influenced by the type of forest species (H = 80.189; p = 0.000; n = 134). As for Hg/C ratio, the highest values of the Hg/N ratio were found in the samples from *P. menziesii* plots, ranging from 10.3 µg Hg g^{-1} N in the OL layers to 19.7 µg Hg g^{-1} N in the OH subhorizons, twice as those for the plots dominated by the native species (QP). In the organic horizons collected from the *Q. pyrenaica* plots were observed the lowest mean values of the Hg/N ratio (Fig. 2), which ranged from 5.1 to 8.7 µg Hg g^{-1} N in the OL and OH subhorizons, respectively. In the samples from the plots of *P. nigra*, the values of the Hg/N ratio were intermediate with a range of 7.8–9.9 µg Hg g^{-1} N (Fig. 2). The type of organic subhorizon was a significant factor of variance for the Hg/N ratio for each tree species, increasing following the sequence abovementioned for the Hg/C ratio.

Regarding to the Hg/S ratio, mean values also varied significantly depending on the type of forest species (H = 75.628; p = 0.000; n = 134). The ranges for the mean values of the Hg/S ratio were 52–88 µg Hg g^{-1} S in *Q. pyrenaica* plots, 72–94 µg Hg g^{-1} S in *P. nigra* plots, and the highest ones were observed in *P. menziesii* plots with values almost twice of those for *Q. pyrenaica* (99–185 µg Hg g^{-1} S). Once again, the type of organic subhorizon was a factor of variance of the Hg/S ratio for each tree species and it increased from the OL to the OH layers (Fig. 2). The increase of the Hg/S ratio from OL to OH subhorizons was 1.9, 1.3 and 1.7 times for PM, PN and QP plots, respectively.

4. Discussion

4.1. General characterization of the organic horizons

The proximity between sampling plots minimizes the influence of factors such as parent material, soil texture, climate and geomorphology. Therefore, the variations in the chemical characteristics among the organic horizons are mainly attributed to species-specific effects, as evidenced in previous studies (Vesterdal et al., 2013; Augusto et al., 2015; Cremer et al., 2016; Lorenz et al., 2020).

The C/N ratio of the organic horizons studied in Serra da Nogueira was within the range (16–44) reported in European forests (Cools et al., 2014). Higher values of the C/N ratio in the organic horizons of coniferous plots (PN and PM) (Table 1), were in agreement with a lower degree of organic
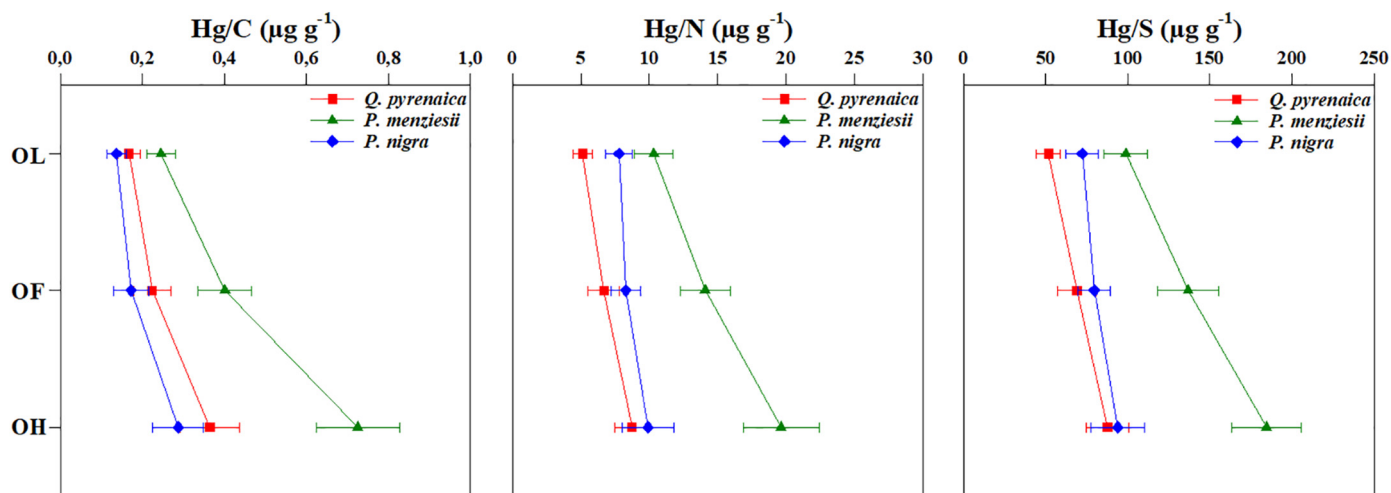

Fig. 2. Mean (symbols) and standard deviation (error bars) of the Hg/C, Hg/N and Hg/S ratios in the soil organic subhorizons (OL, OF and OH) of plots covered by different tree species.

matter decomposition (Díaz-Pinés et al., 2011; Augusto et al., 2015; Lorenz et al., 2020; Güner et al., 2021). On the contrary, the higher content of total N in the organic horizons under the native species (QP) could be justified by a faster organic matter decomposition, resulting in a lower C/N ratio (Vesterdal et al., 2012). Differences in the C/N ratio among species are also reasonable, as the chemical composition of the organic horizons biomass is species-specific (Augusto et al., 2002; Vesterdal et al., 2008). Similarly to that reported by Fonseca et al. (2019), a larger accumulation of total organic C in O horizons under coniferous species compared to the deciduous was also observed in previous studies (Prescott et al., 2000; Díaz-Pinés et al., 2011; Prietzel and Bachmann, 2012; Grüneberg et al., 2014).

Regarding the type of organic subhorizon, the progressive reduction of the C/N ratio from the OL to the OH (Table 1) was in agreement with the more fresh material and lignin-rich biomass in the former (Cools et al., 2014; López-Marcos et al., 2018). Total organic C and total N in the organic subhorizons sometimes peak in the OF layers departing from the sequence OL > OF > OH often reported in the literature (Herrero et al., 2016; Lorenz et al., 2020). However, highest values of total N in the OF layer of forest soils dominated by coniferous or deciduous species have already been observed in other studies, varying between 12 and 25 g kg^{-1} and being similar to ours (Hilli et al., 2008; Trum et al., 2011).

The lower values of pHw in the organic horizons of *P. nigra* plots, compared to the native species (QP), were in agreement with previous studies and attributed to a slower decomposition of organic matter and greater organic acidity in soils under coniferous species (Augusto et al., 2002; Gartzia-Bengoetxea et al., 2009; Cremer and Prietzel, 2017). The abundance of exchangeable base cations was also affected by the dominant tree species through their different chemical composition of litterfall (Augusto et al., 2002; Hansen et al., 2009; Cools et al., 2014; Cremer and Prietzel, 2017).

4.2. Total Hg in the organic horizons: concentrations and pools

The average total Hg content (Hg$_T$) in the organic horizons of Serra da Nogueira plots (110 µg kg^{-1}) was about half of the mean contents (200 µg kg^{-1}) in the humus layers of forest soils across Europe reported by Salminen et al. (2005), suggesting that the study area is exposed to a low degree of Hg diffuse pollution. Total Hg in the O layers (50–214 µg kg^{-1}; Fig. 1) was also in the range reported for these horizons in temperate and subtropical forest soils worldwide not affected by Hg emission point sources (Obrist et al., 2009, 2011; Juillerat et al., 2012; Navrátil et al., 2014; Yu et al., 2014; Richardson and Friedland, 2015; Zhou et al., 2015; Gerson et al., 2017; Gruba et al., 2019).

The different Hg$_T$ contents in the O horizons among tree species in Serra da Nogueira could be explained by the abovementioned behavior of soil organic matter (C/N ratio), as well as the influence of species-specific characteristics (Richardson and Friedland, 2015). The higher concentrations of Hg$_T$ in the organic horizons of the coniferous plots (specially in *P. menziesii*) compared to deciduous plots (Fig. 1), agree with the recent findings of Ballabio et al. (2021), who reported greater Hg$_T$ concentrations in topsoils from coniferous than for deciduous species in an extensive study across Europe. Previous works also showed greater Hg$_T$ concentrations in the O horizons under coniferous species than deciduous ones (Obrist et al., 2012; Blackwell and Driscoll, 2015a; Richardson and Friedland, 2015; Návratil et al., 2016; Gruba et al., 2019).

Soil organic matter parameters, such as total organic C or total N, only correlated to Hg$_T$ in the plots under *Q. pyrenaica* (weakly correlation) and *P. nigra*, respectively (Table S3). This contrasts in some extent with previous studies that showed a close relationship between total organic C and Hg$_T$ in the O horizons of forest soils (Demers et al., 2007; Obrist et al., 2009, 2012; Gong et al., 2014; Navrátil et al., 2014; Wang et al., 2016b; Zhou et al., 2017). Nevertheless, when the degree of organic matter decomposition was considered and C/N ratio was used as proxy, there was a close correlation with Hg$_T$ in the organic horizons for all plots (Table S3). This suggests that, rather than a quantitative factor (soil organic C and N), it is a qualitative factor (C/N ratio) responsible for the variation of Hg$_T$ in the organic

horizons among different tree species. Therefore, a slower organic matter decomposition rate (high C/N ratios) would contribute to higher Hg$_T$ concentrations in the plots dominated by coniferous species as suggested by Blackwell and Driscoll (2015a). The rate of organic matter decomposition was reported to be influenced by the foliar composition and nutritional content such as lignin, C and N and base cations (Prescott et al., 2000). In this context, slower decomposition rate in needles was attributed to their higher lignin and lower N content, becoming less suitable for microbial decomposition, which may favor Hg retention in organic horizons originated under coniferous species (Zhou et al., 2018).

Beyond the organic matter dynamics, species-specific traits could also contribute to the higher Hg$_T$ values in the organic horizons under coniferous species. Indeed, characteristics such as canopy morphology, roughness, greater foliar surface and needle longevity were found to favor a greater Hg accumulation in areas with coniferous than with deciduous species (Hall and St. Louis, 2004; Juillerat et al., 2012; Obrist et al., 2012; Blackwell and Driscoll, 2015a; Zhou et al., 2017). The shorter life-span of *P. nigra* needles compared to those of *P. menziesii* (average of 3 and 6–8 yr, respectively) provides the needles of the latter a longer period to uptake Hg from air masses and, consequently, a potential greater transfer of Hg to the organic horizons through litterfall. In fact, Blackwell and Driscoll (2015b) considered needle age a key factor in Hg accumulation in coniferous species.

The increasing trend of Hg$_T$ from OL to OF and OH subhorizons (Fig. 1) can be related to their different organic matter decomposition degree, which leads to a faster loss of C upon Hg during its humification (Hall and St. Louis, 2004; Demers et al., 2007; Pokharel and Obrist, 2011; Wang et al., 2016b). An efficient immobilization of both N and Hg as litter decomposition progresses (Obrist et al., 2009), or a greater adsorption capacity of the atmospherically deposited Hg in the more humified OF and OH subhorizons (Obrist et al., 2009; Pokharel and Obrist, 2011; Obrist et al., 2011), could also contribute to the trend showed by Hg$_T$ among organic subhorizons. These mechanisms would justify the peaks of Hg$_T$ in the OH layers at all plots from Serra da Nogueira, coinciding with what was observed in previous studies (Åkerblom et al., 2008; Obrist et al., 2009; Gong et al., 2014; Richardson and Friedland, 2015; Gerson et al., 2017; Zhou et al., 2017).

Mean values of the Hg reservoirs in the whole organic horizons (Hg$_{ResT}$), which varied from 189 to 471 µg m^{-2} (Fig. 1), were greater than the range (43–64 µg m^{-2}) obtained by Zhou et al. (2017) in stands dominated by deciduous or coniferous species in China. On the contrary, our Hg$_{ResT}$ values were considerably lower than those obtained for the organic horizons from other forest stands worldwide (Obrist, 2012; Blackwell et al., 2014; Navrátil et al., 2014, 2016; Yu et al., 2014; Richardson and Friedland, 2015; Wang et al., 2016b; Gruba et al., 2019), confirming the low exposure to atmospheric Hg loads at Serra da Nogueira.

The higher Hg$_{Res}$ in the organic horizons of the coniferous plots (Fig. 1) are consistent with previous studies reporting higher Hg pools in coniferous stands as compared to deciduous ones (Stankwitz et al., 2012; Richardson and Friedland, 2015; Gerson et al., 2017; Gruba et al., 2019). Mercury and organic C accumulation in the organic horizons of Serra da Nogueira are strongly dependent on the basis of the close correlations between Hg$_{Res}$ and the reservoir of total organic C (C$_{Res}$) for each species (Table S3), a fact that was also indicated by Juillerat et al. (2012) and Navrátil et al. (2016). Ballabio et al. (2021) also pointed out a close relationship between soil organic matter accumulation and Hg reservoirs in topsoils from Europe. Despite of this findings, other studies did not report significant differences in the Hg$_{Res}$ of organic horizons between deciduous and coniferous forests (Obrist et al., 2012; Zhou et al., 2017) or they even reported higher values in O layers under deciduous species (Demers et al., 2007; Blackwell et al., 2014).

The differences in the Hg$_{Res}$ among the organic subhorizons follow the same trend than their areal mass (Table 1), with a positive correlation for all samples ($rho = 0.914$, $p = 0.000$, $n = 134$) and for each species (Table S3). This is in agreement with Stankwitz et al. (2012) who reported the

influence of the O horizons mass in the reservoirs of several metals in forest soils. Significant correlations between Hg_{Res} and total contents and reservoirs of biophilic elements (C, N, S, C_{Res}, N_{Res} and S_{Res}) and the C/N and C/S ratios were also found (Table S3, Fig. S2). This suggests that the organic matter decomposition degree would account for the differences of Hg_{Res} among organic subhorizons as there are more available sites for Hg retention and storage in the OH subhorizons (Pokharel and Obrist, 2011; Yu et al., 2014; Richardson and Friedland, 2015; Zhou et al., 2017). Previous studies have already pointed out the influence of C, N and S pools in organic horizons as well as the biogeochemical processes involved in the organic matter turnover (Obrist et al., 2009, 2012; Juillerat et al., 2012; Navrátil et al., 2014; Richardson and Friedland, 2015). The influence of dominant tree species in the Hg_{Res} of the organic subhorizons would depend on the organic matter accumulation and decomposition, the concentration of Hg

in each of the organic subhorizons and the aboveground biomass storage as the main source of shed material to the forest floor (Table S4). The joint effect of these factors (i.e. the quantity and quality of the organic matter and the Hg stored in the forest floor and in the aboveground biomass) explains the highest Hg_{Res} in the organic horizons of the *P. menziesii* plots.

4.3. Relationships between Hg and biophilic elements of soil organic matter

The ratios between Hg and biophilic elements are frequently used to assess potential species-specific effects in the occurrence and accumulation of Hg in organic horizons of forest soils (Obrist et al., 2012; Navrátil et al., 2014, 2016; Blackwell and Driscoll, 2015b). The Hg/C ratio in the plots of Serra da Nogueira was within the range (0.4–1.7 µg Hg g^{-1}C) reported
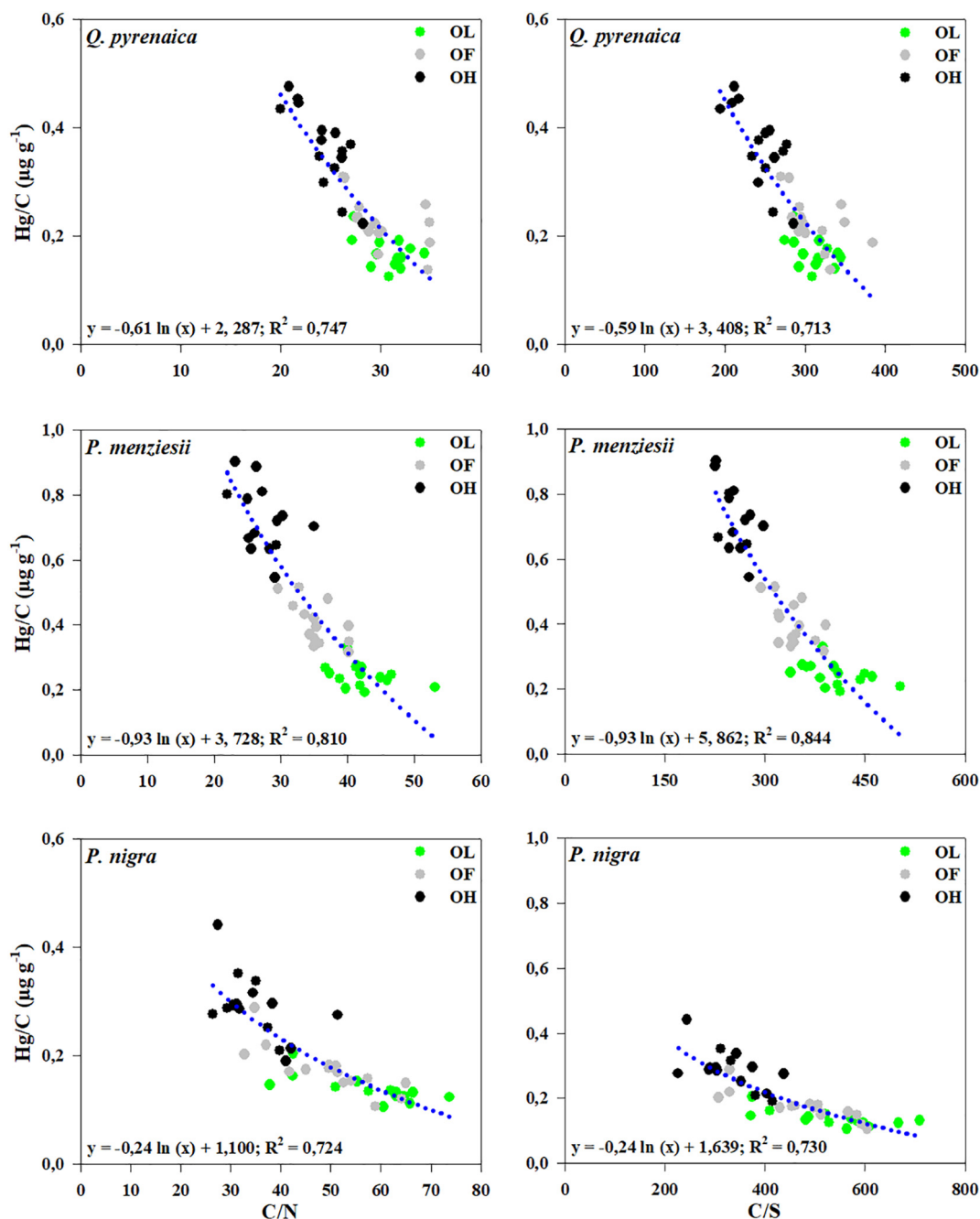

Fig. 3. Relationships of Hg/C ratio with C/N and C/S ratios in the organic subhorizons of plots covered by different tree species. Trend line (dotted) fitted to data for all organic subhorizons.

for organic horizons of forest soils from Canada, USA and Europe (Nasr and Arp, 2011; Juillerat et al., 2012; Obrist et al., 2009; Obrist et al., 2012; Navrátil et al., 2014; Gruba et al., 2019).

The increase of Hg/C ratio with the progressive decay of soil organic matter in the organic horizons, i.e. from OL to OH subhorizons, took place in all studied plots of Serra da Nogueira (Fig. 2), in parallel to the decrease of organic matter decomposition proxies such as the C/N and C/S ratios (Table 1, Fig. 3). Indeed, the Hg/C and the C/N and C/S ratios correlated negative and significantly for all tree species (Table S5), coinciding with what was reported in forest soils worldwide (Obrist et al., 2011; Juillerat et al., 2012; Navrátil et al., 2014, 2016; Yu et al., 2014; Blackwell and Driscoll, 2015b). A possible explanation for the trend of the Hg/C ratio in the studied organic subhorizons could be a larger availability of Hg binding sites as organic matter decomposes (Amirbahman and Fernandez, 2012; Demers et al., 2007), making Hg less prone to revolatilization from the more humified layers (Yu et al., 2014), and/or a longer exposure to Hg atmospheric deposition as the OF and OH layers get older (Obrist et al., 2009, 2011).

The Hg/N and Hg/S ratios (Fig. 2) also increased with the course of organic matter decomposition as previous studies had also shown (Obrist et al., 2009; Navrátil et al., 2014; Demers et al., 2013; Gerson et al., 2017), being attributed to a slower release of N and S than C during organic matter decomposition (Demers et al., 2007; Navrátil et al., 2014). Present values for the Hg/N ratio were similar to those found in coniferous forests from the USA (4.7–11.6 μg Hg g^{-1} N; Obrist et al., 2009), but they expressively fall out of the range 12–35 μg Hg g^{-1} N reported in coniferous forest soils from the Czech Republic (Navrátil et al., 2014). The relevance of functional groups of organic N in the retention of Hg can explain the close correlations of Hg$_{Res}$ and N reservoirs at Serra da Nogueira (Table S3) as Obrist et al. (2009) highlighted. The Hg/S ratio in Serra da Nogueira was similar to the range 83–188 μg Hg g^{-1} S found in previous studies (Nasr and Arp, 2011; Navrátil et al., 2014). The existence of favorable conditions to S immobilization as organic matter decomposes could also contribute to Hg accumulation in O horizons due to the high affinity of Hg and reduced S species (Skyllberg et al., 2006; Wang et al., 2016b). On this basis, the organic subhorizons with the lower C/S ratios (OH layers) corresponded to those with the higher Hg/S ratios and, consequently, with the highest values of Hg$_T$ (Figs. 1 and 3).

The Hg/C, Hg/N and Hg/S ratios were significantly different among species (Table S6) and decreased following the sequence *P. menziesii* > *P. nigra* $\geq$ *Q. pyrenaica* (Fig. 2), consistent with Hg$_T$ and Hg$_{Res}$ values (Fig. 1). Pokharel and Obrist (2011) also found that the Hg/C ratio in organic horizons differed depending on the tree species. Supporting our findings, greater values of the Hg/C and Hg/N ratios in forest floor samples of coniferous than in deciduous stands were also reported previously (Obrist et al., 2012; Navrátil et al., 2016; Gerson et al., 2017). The species-specific variations in the C/N and C/S ratios of the organic horizons (Table S6) suggest that organic matter decomposition would influence the stoichiometric ratios between Hg and biophilic elements (C, N and S), justifying the differences of Hg$_T$ and Hg$_{Res}$ among tree species in plots from Serra da Nogueira. Despite the similarity of the C/N and C/S ratios between *P. menziesii* and *Q. pyrenaica* (Fig. S1), the organic horizons of the former species stored 46–76% more Hg. A better efficiency of *P. menziesii* than *P. nigra* and *Q. pyrenaica* in the scavenging of atmospheric Hg would imply a greater Hg enrichment in the organic horizons of the former species. In this sense, the accumulation of Hg in the organic horizons of forest soils is species-specific and built on both post-depositional processes affecting Hg dynamics (mostly organic matter decomposition) and the pathways of atmospheric Hg deposition (litterfall and throughfall).

4.4. Implications of forest management in environmental Hg dynamics

The afforestation in Serra da Nogueira with coniferous species (*P. menziesii* and *P. nigra*) could lead to undesirable effects related to Hg accumulation, a fact that must be considered during forest management

plans. The greater accumulation of Hg showed by the organic horizons of coniferous species plots would increase the risks of Hg mobilization through runoff and methyl-Hg production as was observed in previous studies assessing the consequences of forestry practices (Porvari et al., 2003; Mitchell et al., 2012; Eckley et al., 2018; Eklöf et al., 2018). The increase of Hg availability during organic matter decomposition, reported during the first years after logging (Skyllberg et al., 2009; Zhang et al., 2016), became an environmental issue of concern in those plots where a greater accumulation of organic matter and Hg occur such as those dominated by coniferous species. Due to a greater Hg (and methyl-Hg) availability after timber harvesting as was outlined by Willacker et al. (2019), damages in the food web and headwater quality would be expected in Serra da Nogueira after the exploitation of the afforested areas. Headwater mountain streams from Serra da Nogueira feed downstream areas associated to the Douro river plains where there are high population densities and intense socioeconomic activities. Therefore, decisions on forest management practices may have consequences beyond those initially and typically considered.

On the other hand, considering that a substantial fraction of Hg accumulated in the organic horizons can be volatilized during wildfires (Friedli et al., 2009; Webster et al., 2016), the greater organic matter accumulation in the plots of Serra da Nogueira dominated by coniferous species also supposes a higher supply of Hg to be released in case of fire. This is an additional environmental risk in the study area, as the impact of tree species substitution in the organic C pools and forest soil sustainability were previously reported by Fonseca et al. (2019).

According to Zhou et al. (2017), the potential Hg emission due to wildfires is equivalent to the Hg$_{ResT}$ in the organic horizons, therefore the burning of organic horizons in *Q. pyrenaica*, *P. menziesii* and *P. nigra* plots would release 189, 471 and 253 μg Hg m^{-2}, respectively. Thus, the Hg emitted to the atmosphere during a wildfire in PM and PN plots would be up to 1.5 and 0.3 times greater than in those dominated by the native species (QP), respectively. Although with some uncertainties, potential Hg emissions due to wildfires in Serra da Nogueira (189–471 μg Hg m^{-2}) would be quite similar to the range 150–640 μg Hg m^{-2} reported in some studies carried out in the Northern hemisphere (Engle et al., 2006; Wiedinmyer and Friedli, 2007). As the study area is prone to undergo frequent wildfires as a consequence of climate change (Turco et al., 2019), caution is desirable when tree species are selected to afforestation with the aim of minimize the amount of Hg in organic horizons liable to volatilization.

5. Conclusions

The type of forest species in the study area rise up as a driving factor influencing the contents and reservoir of mercury in the organic horizons of the forest soils. Moreover, the strong correlations between Hg$_T$ and the C/N ratio suggest that Hg accumulation was more influenced by the organic matter quality than its quantity. The organic matter quality, approached by C/N and C/S ratios, also determine the patterns of Hg concentrations and reservoirs among organic subhorizons (OL, OF and OH) which are consistent with the progressive humification they show. However, tree canopy characteristics also can influence Hg contents in the organic horizons through their distinctive efficiency in the capture of atmospheric Hg. The joint effect of a greater efficiency in the uptake of atmospheric Hg and a moderate organic matter decomposition degree point out to *P. menziesii* as the species that contributes the most to Hg accumulation in the organic horizons of the forest soils in Serra da Nogueira.

Although fast-growing coniferous species (*P. nigra* and *P. menziesii*) contributed to the role of soil organic horizons as Hg sink in a greater extent than the deciduous native species (*Q. pyrenaica*), this advantage is not free of charge. Thus, a greater Hg accumulation also implies more risks of future Hg mobilization associated with forest management activities or wildfires. In this regard, forest management plans should consider the selection of a suitable tree species for afforestation as a key point, taking into account commercial exploitation and environmental consequences derived from the modification of the biogeochemical cycles of elements and, particularly, of highly toxic contaminants such as Hg.

CRediT authorship contribution statement

M. Méndez-López: Conceptualization, Methodology, Data curation, Visualization, Formal analysis, Investigation, Writing – original draft, Writing – review & editing. **A. Gómez-Armesto:** Methodology, Data curation, Formal analysis, Investigation, Writing – original draft, Writing – review & editing. **F. Alonso-Vega:** Writing – original draft, Funding acquisition, Resources, Visualization, Supervision, Writing – review & editing. **X. Pontevedra-Pombal:** Resources, Visualization, Data curation. **L. Fonseca:** Data curation, Investigation, Visualization, Writing – review & editing. **T. de Figueiredo:** Data curation, Investigation, Visualization, Writing – review & editing. **M. Arias-Estévez:** Funding acquisition, Visualization, Resources, Supervision, Project administration. **J.C. Nóvoa-Muñoz:** Conceptualization, Formal analysis, Visualization, Resources, Writing – original draft, Supervision, Writing – review & editing, Funding acquisition, Project administration.

Declaration of competing interest

The authors declare that they have no known competing financial interests or personal relationships that could have appeared to influence the work reported in this paper.

Acknowledgments

Appendix A. Supplementary data

Supplementary data to this article can be found online at https://doi.org/10.1016/j.scitotenv.2022.154345.

References

Åkerblom, S., Meili, M., Bringmark, L., Johansson, K., Kleja, D.B., Bergkvist, B., 2008. Partitioning of Hg between solid and dissolved organic matter in the humus layer of boreal forests. Water Air Soil Pollut. 189, 239–252. https://doi.org/10.1007/s11270-007-9571-1.

Almeida, M.D., Lacerda, L.D., Bastos, W.R., Herrmann, J.C., 2005. Mercury loss from soils following conversion from forest to pasture in Rondônia, Western Amazon,Brazil. Environ. Pollut. 137, 179–186. https://doi.org/10.1016/j.envpol.2005.02.026.

Amirbahman, A., Fernandez, I.J., 2012. The role of soils in storage and cycling of mercury. Anonymous Mercury in the Environment: Pattern and Process, pp. 99–118.

Augusto, L., Ranger, J., Binkley, D., Rothe, A., 2002. Impact of several common tree species of European temperate forests on soil fertility. Ann. For. Sci. 59, 233–253. https://doi.org/10.1051/forest:2002020.

Augusto, L., De Schrijver, A., Vesterdal, L., Smolander, A., Prescott, C., Ranger, J., 2015. Influences of evergreen gymnosperm and deciduous angiosperm tree species on the functioning of temperate and boreal forests. Biol. Rev. 90, 444–466. https://doi.org/10.1111/brv.12119.

Ballabio, C., Jiskra, M., Osterwalder, S., Borrelli, P., Montanarella, L., Panagos, P., 2021. A spatial assessment of mercury content in the European Union topsoil. Sci. Total Environ. 769. https://doi.org/10.1016/j.scitotenv.2020.144755.

Blackwell, B.D., Driscoll, C.T., 2015a. Deposition of mercury in forests along a montane elevation gradient. Environ. Sci. Technol. 49, 5363–5370. https://doi.org/10.1021/es505928w.

Blackwell, B.D., Driscoll, C.T., 2015b. Using foliar and forest floor mercury concentrations to assess spatial patterns of mercury deposition. Environ. Pollut. 202, 126–134. https://doi.org/10.1016/j.envpol.2015.02.036.

Blackwell, B.D., Driscoll, C.T., Maxwell, J.A., Holsen, T.M., 2014. Changing climate alters inputs and pathways of mercury deposition to forested ecosystems. Biogeochemistry 119, 215–228. https://doi.org/10.1007/s10533-014-9961-6.

Carpi, A., Fostier, A.H., Orta, O.R., dos Santos, J.C., Gittings, M., 2014. Gaseous mercury emissions from soil following forest loss and land use changes: field experiments in the United States and Brazil. Atmos. Environ. 96, 423–429. https://doi.org/10.1016/j.atmosenv.2014.08.004.

Cools, N., Vesterdal, L., De Vos, B., Vanguelova, E., Hansen, K., 2014. Tree species is the major factor explaining C: N ratios in European forest soils. For. Ecol. Manag. 311, 3–16. https://doi.org/10.1016/j.foreco.2013.06.047.

Cremer, M., Prietzel, J., 2017. Soil acidity and exchangeable base cation stocks under pure and mixed stands of European beech, Douglas fir and Norway spruce. Plant Soil 415, 393–405. https://doi.org/10.1007/s11104-017-3177-1.

Cremer, M., Kern, N.V., Prietzel, J., 2016. Soil organic carbon and nitrogen stocks under pure and mixed stands of European beech, Douglas fir and Norway spruce. For. Ecol. Manag. 367, 30–40. https://doi.org/10.1016/j.foreco.2016.02.020.

Demers, J.D., Driscoll, C.T., Fahey, T.J., Yavitt, J.B., 2007. Mercury cycling in litter and soil in different forest types in the adirondack region, New York,USA. Ecol. Appl. 17, 1341–1351. https://doi.org/10.1890/06-1697.1.

Demers, J.D., Blum, J.D., Zak, D.R., 2013. Mercury isotopes in a forested ecosystem: Implications for air-surface exchange dynamics and the global mercury cycle. Global Biogeochem. Cycles 27 (1), 222–238.

Díaz-Pinés, E., Rubio, A., Van Miegroet, H., Montes, F., Benito, M., 2011. Does tree species composition control soil organic carbon pools in Mediterranean mountain forests? For. Ecol. Manag. 262, 1895–1904. https://doi.org/10.1016/j.foreco.2011.02.004.

Eckley, C.S., Eagles-Smith, C., Tate, M.T., Kowalski, B., Danehy, R., Johnson, S.L., Krabbenhoft, D.P., 2018. Stream mercury export in response to contemporary timber harvesting methods (Pacific Coastal Mountains, Oregon, USA). Environ. Sci. Technol. 52, 1971–1980. https://doi.org/10.1021/acs.est.7b05197.

Eklöf, K., Bishop, K., Bertilsson, S., Björn, E., Buck, M., Skyllberg, U., Osman, O.A., Kronberg, R., Bravo, A.G., 2018. Formation of mercury methylation hotspots as a consequence of forestry operations. Sci. Total Environ. 613–614, 1069–1078. https://doi.org/10.1016/j.scitotenv.2017.09.151.

Engle, M.A., Gustin, M.S., Johnson, D.W., Murphy, J.F., Miller, W.W., Walker, R.F., Wright, J., Markee, M., 2006. Mercury distribution in two Sierran forest and one desert sagebrush steppe ecosystems and the effects of fire. Sci. Total Environ. 367, 222–233. https://doi.org/10.1016/j.scitotenv.2005.11.025.

Fonseca, F., de Figueiredo, T., Vilela, Â., Santos, R., de Carvalho, A., Almeida, E., Nunes, L., 2019. Impact of tree species replacement on carbon stocks in a Mediterranean mountain area, NE Portugal. For. Ecol. Manag. 439, 181–188. https://doi.org/10.1016/j.foreco.2019.03.002.

Friedli, H.R., Arellano, A.F., Cinnirella, S., Pirrone, N., 2009. Initial estimates of mercury emissions to the atmosphere from global biomass burning. Environ. Sci. Technol. 43, 3507–3513. https://doi.org/10.1021/es802703g.

Gartzia-Bengoetxea, N., González-Arias, A., de Arano, I.M., 2009. Effects of tree species and clear-cut forestry on forest-floor characteristics in adjacent temperate forests in northern Spain. Can. J. For. Res. 39, 1302–1312. https://doi.org/10.1139/X09-053.

Gerson, J.R., Driscoll, C.T., Demers, J.D., Sauer, A.K., Blackwell, B.D., Montesdeoca, M.R., Shanley, J.B., Ross, D.S., 2017. Deposition of mercury in forests across a montane elevation gradient: elevational and seasonal patterns in methylmercury inputs and production. J. Geophys. Res. Biogeosci. 122, 1922–1939. https://doi.org/10.1002/2016JG003721.

Gómez-Armesto, A., Méndez-López, M., Pérez-Rodríguez, P., Fernández-Calviño, D., Arias-Estévez, M., Nóvoa-Muñoz, J., 2020a. Litterfall hg deposition to an oak forest soil from southwestern Europe. J. Environ. Manag. 269, 110858. https://doi.org/10.1016/j.jenvman.2020.110858.

Gómez-Armesto, A., Martínez-Cortizas, A., Ferro-Vázquez, C., Méndez-López, M., Arias-Estévez, M., Nóvoa-Muñoz, J.C., 2020b. Modelling Hg mobility in podzols: role of soil components and environmental implications. Environ. Pollut. 260. https://doi.org/10.1016/j.envpol.2020.114040.

Gong, P., Wang, X., Xue, Y., Xu, B., Yao, T., 2014. Mercury distribution in the foliage and soil profiles of the Tibetan forest: processes and implications for regional cycling. Environ. Pollut. 188, 94–101. https://doi.org/10.1016/j.envpol.2014.01.020.

Gottfried, M., Pauli, H., Futschik, A., Akhalkatsi, M., Barančok, P., Benito Alonso, J.L., Coldea, G., Dick, J., Erschbamer, B., Fernández Calzado, M.R., Kazakis, G., Krajči, J., Larsson, P., Mallaun, M., Michelsen, O., Moiseev, D., Moiseev, P., Molau, U., Merzouki, A., Nagy, L., Nakhutsrishvili, G., Pedersen, B., Pelino, G., Puscas, M., Rossi, G., Stanisci, A., Theurillat, J., Tomaselli, M., Villar, L., Vittoz, P., Vogiatzakis, I., Grabherr, G., 2012. Continent-wide response of mountain vegetation to climate change. Nat. Clim. Change 2, 111–115. https://doi.org/10.1038/nclimate1329.

Gruba, P., Socha, J., Pietrzykowski, M., Pasychnyk, D., 2019. Tree species affects the concentration of total mercury (Hg) in forest soils: evidence from a forest soil inventory in Poland. Sci. Total Environ. 647, 141–148. https://doi.org/10.1016/j.scitotenv.2018.07.452.

Grüneberg, E., Ziche, D., Wellbrock, N., 2014. Organic carbon stocks and sequestration rates of forest soils in Germany. Glob. Chang. Biol. 20, 2644–2662. https://doi.org/10.1111/gcb.12558.

Guedron, S., Grangeon, S., Lanson, B., Grimaldi, M., 2009. Mercury speciation in a tropical soil association; consequence of gold mining on Hg distribution in French Guiana. Geoderma 153, 331–346. https://doi.org/10.1016/j.geoderma.2009.08.017.

Guiot, J., Cramer, W., 2016. Climate change: the 2015 Paris agreement thresholds and Mediterranean basin ecosystems. Science 354, 465–468. https://doi.org/10.1126/science.aah5015.

Güner, Ş.T., Erkan, N., Karataş, R., 2021. Effects of afforestation with different species on carbon pools and soil and forest floor properties. Catena 196. https://doi.org/10.1016/j.catena.2020.104871.

Hall, B.D., St. Louis, V.L., 2004. Methylmercury and total mercury in plant litter decomposing in upland forests and flooded landscapes. Environ. Sci. Technol. 38, 5010–5021. https://doi.org/10.1021/es049800q.

Hansen, K., Vesterdal, L., Schmidt, I.K., Gundersen, P., Sevel, L., Bastrup-Birk, A., Pedersen, L.B., Bille-Hansen, J., 2009. Litterfall and nutrient return in five tree species in a common garden experiment. For. Ecol. Manag. 257, 2133–2144. https://doi.org/10.1016/j.foreco.2009.02.021.

Herrero, C., Turrión, M.B., Pando, V., Bravo, F., 2016. Carbon content of forest floor and mineral soil in Mediterranean pinus spp. and Oak stands in acid soils in Northern Spain. For. Syst. 25 (doi:10.5424/fs/2016252-09149).

Hilli, S., Stark, S., Derome, J., 2008. Carbon quality and stocks in organic horizons in boreal forest soils. Ecosystems 11, 270–282. https://doi.org/10.1007/s10021-007-9121-0.

IUSS Working Group WRB, 2015. World Reference Base for Soil Resources 2014, update 2015. International soil classification system for naming soils and creating legends for soil maps. World Soil Resources Reports, 106, FAO, Rome.

Jiskra, M., Sonke, J.E., Obrist, D., Bieser, J., Ebinghaus, R., Myhre, C.L., Pfaffhuber, K.A., Wängberg, I., Kyllönen, K., Worthy, D., Martin, L.G., Labuschagne, C., Mkololo, T., Ramonet, M., Magand, O., Dommergue, A., 2018. A vegetation control on seasonal variations in global atmospheric mercury concentrations. Nat. Geosci. 11, 244–250. https://doi.org/10.1038/s41561-018-0078-8.

Juillerat, J.I., Ross, D.S., Bank, M.S., 2012. Mercury in litterfall and upper soil horizons in forested ecosystems in Vermont, USA. Environ. Toxicol. Chem. 31, 1720–1729 doi.

Kumar, A., Wu, S., Huang, Y., Liao, H., Kaplan, J.O., 2018. Mercury from wildfires: global emission inventories and sensitivity to 2000–2050 global change. Atmos. Environ. 173, 6–15. https://doi.org/10.1002/etc.1896.

Lindner, M., Maroschek, M., Netherer, S., Kremer, A., Barbati, A., Garcia-Gonzalo, J., Seidl, R., Delzon, S., Corona, P., Kolström, M., Lexer, M.J., Marchetti, M., 2010. Climate change impacts, adaptive capacity, and vulnerability of European forest ecosystems. For. Ecol. Manag. 259, 698–709. https://doi.org/10.1016/j.foreco.2009.09.023.

López-Marcos, D., Martínez-Ruiz, C., Turrión, M., Jonard, M., Titeux, H., Ponette, Q., Bravo, F., 2018. Soil carbon stocks and exchangeable cations in monospecific and mixed pine forests. Eur. J. For. Res. 137, 831–847. https://doi.org/10.1007/s10342-018-1143-y.

Lorenz, M., Derrien, D., Zeller, B., Udelhoven, T., Werner, W., Thiele-Bruhn, S., 2020. The linkage of 13C and 15N soil depth gradients with C:N and O:C stoichiometry reveals tree species effects on organic matter turnover in soil. Biogeochemistry 151, 203–220. https://doi.org/10.1007/s10533-020-00721-3.

Ma, M., Du, H., Wang, D., 2019. A new perspective is required to understand the role of forest ecosystems in global mercury cycle: a review. Bull. Environ. Contam. Toxicol. 102, 650–656. https://doi.org/10.1007/s00128-019-02569-2.

Mitchell, C.P.J., Kolka, R.K., Fraver, S., 2012. Singular and combined effects of blowdown, salvage logging, and wildfire on forest floor and soil mercury pools. Environ. Sci. Technol. 46, 7963–7970. https://doi.org/10.1021/es300133h.

Mosbæk, H., Tjell, J.C., Sevel, T., 1988. Plant uptake of airborne mercury in background areas. Chemosphere 17, 1227–1236. https://doi.org/10.1016/0045-6535(88)90189-0.

Nasr, M., Arp, P.A., 2011. Hg concentrations and accumulations in fungal fruiting bodies, as influenced by forest soil substrates and moss carpets. Appl. Geochem. 26, 1905–1917. https://doi.org/10.1016/j.apgeochem.2011.06.014.

Navrátil, T., Shanley, J., Rohovec, J., Hojdová, M., Penížek, V., Buchtová, J., 2014. Distribution and pools of mercury in Czech forest soils. Water Air Soil Pollut. 225. https://doi.org/10.1016/j.gexplo.2021.106782.

Navrátil, T., Shanley, J.B., Rohovec, J., Oulehle, F., Šimecek, M., Houška, J., Cudlín, P., 2016. Soil mercury distribution in adjacent coniferous and deciduous stands highly impacted by acid rain in the Ore Mountains, Czech Republic. Appl. Geochem. 75, 63–75. https://doi.org/10.1016/j.apgeochem.2016.10.005.

Navrátil, T., Nováková, T., Roll, M., Shanley, J.B., Kopáček, J., Rohovec, J., Kaňa, J., Cudlín, P., 2019. Decreasing litterfall mercury deposition in central European coniferous forests and effects of bark beetle infestation. Sci. Total Environ. 682, 213–225. https://doi.org/10.1016/j.scitotenv.2019.05.093.

Obrist, D., 2012. Mercury distribution across 14 U.S. forests. Part II: patterns of methyl mercury concentrations and areal mass of total and methyl mercury. Environ. Sci. Technol. 46, 5921–5930. https://doi.org/10.1021/es3022655.

Obrist, D., Johnson, D.W., Lindberg, S.E., 2009. Mercury concentrations and pools in four Sierra Nevada forest sites, and relationships to organic carbon and nitrogen. Biogeosciences 6, 765–777. https://doi.org/10.5194/bg-6-765-2009.

Obrist, D., Johnson, D.W., Lindberg, S.E., Luo, Y., Hararuk, O., Bracho, R., Battles, J.J., Dail, D.B., Edmonds, R.L., Monson, R.K., Ollinger, S.V., Pallardy, S.G., Pregitzer, K.S., Todd, D.E., 2011. Mercury distribution across 14 U.S. Forests. Part I: spatial patterns of concentrations in biomass, litter, and soils. Environ. Sci. Technol. 45, 3974–3981. https://doi.org/10.1021/es104384m.

Obrist, D., Johnson, D.W., Edmonds, R.L., 2012. Effects of vegetation type on mercury concentrations and pools in two adjacent coniferous and deciduous forests. J. Plant Nutr. Soil Sci. 175, 68–77. https://doi.org/10.1002/jpln.201000415.

Obrist, D., Pearson, C., Webster, J., Kane, T., Lin, C., Aiken, G.R., Alpers, C.N., 2016. A synthesis of terrestrial mercury in the western United States: spatial distribution defined by land cover and plant productivity. Sci. Total Environ. 568, 522–535. https://doi.org/10.1016/j.scitotenv.2015.11.104.

Obrist, D., Kirk, J.L., Zhang, L., Sunderland, E.M., Jiskra, M., Selin, N.E., 2018. A review of global environmental mercury processes in response to human and natural perturbations: changes of emissions, climate, and land use. Ambio 47, 116–140. https://doi.org/10.1007/s13280-017-1004-9.

Peña-Rodríguez, S., Pontevedra-Pombal, X., Gayoso, E.G.R., Moretto, A., Mansilla, R., Cutillas-Barreiro, L., Arias-Estévez, M., Nóvoa-Muñoz, J.C., 2014. Mercury distribution in a toposequence of sub-Antarctic forest soils of Tierra del Fuego (Argentina) as consequence of the prevailing soil processes. Geoderma 232–234, 130–140. https://doi.org/10.1016/j.geoderma.2014.04.040.

Pokharel, A.K., Obrist, D., 2011. Fate of mercury in tree litter during decomposition. Biogeosciences 8, 2507–2521. https://doi.org/10.5194/bg-8-2507-2011.

Porvari, P., Verta, M., Munthe, J., Haapanen, M., 2003. Forestry practices increase mercury and methyl mercury output from boreal forest catchments. Environ. Sci. Technol. 37, 2389–2393. https://doi.org/10.1021/es0340174.

Prescott, C.E., Zabek, L.M., Staley, C.L., Kabzems, R., 2000. Decomposition of broadleaf and needle litter in forests of British Columbia: influences of litter type, forest type, and litter mixtures. Can. J. For. Res. 30, 1742–1750. https://doi.org/10.1139/x00-097.

Prietzel, J., Bachmann, S., 2012. Changes in soil organic C and N stocks after forest transformation from Norway spruce and Scots pine into Douglas fir, Douglas fir/spruce, or

European beech stands at different sites in Southern Germany. For. Ecol. Manag. 269, 134–148. https://doi.org/10.1016/j.foreco.2011.12.034.

Richardson, J.B., Friedland, A.J., 2015. Mercury in coniferous and deciduous upland forests in northern New England, USA: implications of climate change. Biogeosciences 12, 6737–6749. https://doi.org/10.5194/bg-12-6737-2015.

Rutter, A.P., Schauer, J.J., Shafer, M.M., Creswell, J.E., Olson, M.R., Robinson, M., Collins, R.M., Parman, A.M., Katzman, T.L., Mallek, J.L., 2011. Dry deposition of gaseous elemental mercury to plants and soils using mercury stable isotopes in a controlled environment. Atmos. Environ. 45, 848–855. https://doi.org/10.1016/j.atmosenv.2010.11.025.

Salminen, R., Batista, M.J., Bidovec, M., Demetriades, A., De Vivo, B., De Vos, W., Duris, M., et al., 2005. Geochemical Atlas of Europe. Part 1—Background Information, Methodology and Maps. Geological Survey of Finland, Espoo.

Schroeder, W.H., Munthe, J., 1998. Atmospheric mercury - an overview. Atmos. Environ. 32, 809–822. https://doi.org/10.1016/S1352-2310(97)00293-8.

Skyllberg, U., Bloom, P.R., Qian, J., Lin, C., Bleam, W.F., 2006. Complexation of mercury (II) in soil organic matter: EXAFS evidence for linear two-coordination with reduced sulfur groups. Environ. Sci. Technol. 40, 4174–4180. https://doi.org/10.1021/es0600577.

Skyllberg, U., Westin, M.B., Meili, M., Björn, E., 2009. Elevated concentrations of methyl mercury in streams after forest clear-cut: a consequence of mobilization from soil or new methylation? Environ. Sci. Technol. 43, 8535–8541. https://doi.org/10.1021/es900996z.

Smith-Downey, N.V., Sunderland, E.M., Jacob, D.J., 2010. Anthropogenic impacts on global storage and emissions of mercury from terrestrial soils: insights from a new global model. J. Geophys. Res. G Biogeosci. 115. https://doi.org/10.1029/2009JG001124.

Stamenkovic, J., Gustin, M.S., 2009. Nonstomatal versus stomatal uptake of atmospheric mercury. Environ. Sci. Technol. 43, 1367–1372. https://doi.org/10.1021/es801583a.

Stankwitz, C., Kaste, J.M., Friedland, A.J., 2012. Threshold increases in soil lead and mercury from tropospheric deposition across an elevational gradient. Environ. Sci. Technol. 46, 8061–8068. https://doi.org/10.1021/es204208w.

Sumner, M.E., Miller, W.P., 1996. Cation Exchange Capacity and Exchange Coefficients. Methods of Soil Analysis: Part 3 Chemical Methods. 5, pp. 1201–1229.

Terres, J., Scacchiafichi, L.N., Wania, A., Ambar, M., Anguiano, E., Buckwell, A., Coppola, A., Gocht, A., Källström, H.N., Pointereau, P., Strijker, D., Visek, L., Vranken, L., Zobena, A., 2015. Farmland abandonment in Europe: identification of drivers and indicators, and development of a composite indicator of risk. Land Use Policy 49, 20–34. https://doi.org/10.1016/j.landusepol.2015.06.009.

Trum, F., Titeux, H., Ranger, J., Delvaux, B., 2011. Influence of tree species on carbon and nitrogen transformation patterns in forest floor profiles. Ann. For. Sci. 68, 837–847. https://doi.org/10.1007/s13595-011-0080-4.

Turco, M., Jerez, S., Augusto, S., Tarín-Carrasco, P., Ratola, N., Jiménez-Guerrero, P., Trigo, R.M., 2019. Climate drivers of the 2017 devastating fires in Portugal. Sci. Rep. 9. https://doi.org/10.1038/s41598-019-50281-2.

Versini, P., Velasco, M., Cabello, A., Sempere-Torres, D., 2013. Hydrological impact of forest fires and climate change in a Mediterranean basin. Nat. Hazards 66, 609–628. https://doi.org/10.1007/s11069-012-0503-z.

Vesterdal, L., Schmidt, I.K., Callesen, I., Nilsson, L.O., Gundersen, P., 2008. Carbon and nitrogen in forest floor and mineral soil under six common European tree species. For. Ecol. Manag. 255, 35–48. https://doi.org/10.1016/j.foreco.2007.08.015.

Vesterdal, L., Elberling, B., Christiansen, J.R., Callesen, I., Schmidt, I.K., 2012. Soil respiration and rates of soil carbon turnover differ among six common European tree species. For. Ecol. Manag. 264, 185–196. https://doi.org/10.1016/j.foreco.2011.10.009.

Vesterdal, L., Clarke, N., Sigurdsson, B.D., Gundersen, P., 2013. Do tree species influence soil carbon stocks in temperate and boreal forests? For. Ecol. Manag. 309, 4–18. https://doi.org/10.1016/j.foreco.2013.01.017.

Wang, X., Bao, Z., Lin, C., Yuan, W., Feng, X., 2016a. Assessment of global mercury deposition through litterfall. Environ. Sci. Technol. 50, 8548–8557. https://doi.org/10.1021/acs.est.5b06351.

Wang, X., Lin, C., Lu, Z., Zhang, H., Zhang, Y., Feng, X., 2016b. Enhanced accumulation and storage of mercury on subtropical evergreen forest floor: implications on mercury budget in global forest ecosystems. J. Geophys. Res. Biogeosci. 121, 2096–2109. https://doi.org/10.1002/2016JG003446.

Wang, X., Yuan, W., Lin, C., Zhang, L., Zhang, H., Feng, X., 2019. Climate and vegetation as primary drivers for global mercury storage in surface soil. Environ. Sci. Technol. 53, 10665–10675. https://doi.org/10.1021/acs.est.9b02386.

Webster, J.P., Kane, T.J., Obrist, D., Ryan, J.N., Aiken, G.R., 2016. Estimating mercury emissions resulting from wildfire in forests of the Western United States. Sci. Total Environ. 568, 578–586. https://doi.org/10.1016/j.scitotenv.2016.01.166.

Wiedinmyer, C., Friedli, H., 2007. Mercury emission estimates from fires: an initial inventory for the United States. Environ. Sci. Technol. 41, 8092–8098. https://doi.org/10.1021/es071289o.

Willacker, J.J., Eagles-Smith, C.A., Kowalski, B.M., Danehy, R.J., Jackson, A.K., Adams, E.M., Evers, D.C., Eckley, C.S., Tate, M.T., Krabbenhoft, D.P., 2019. Timber harvest alters mercury bioaccumulation and food web structure in headwater streams. Environ. Pollut. 253, 636–645. https://doi.org/10.1016/j.envpol.2019.07.025.

Wright, L.P., Zhang, L., Marsik, F.J., 2016. Overview of mercury dry deposition, litterfall, and throughfall studies. Atmos. Chem. Phys. 16, 13399–13416 doi.

Yang, Y., Meng, L., Yanai, R.D., Montesdeoca, M., Templer, P.H., Asbjornsen, H., Rustad, L.E., Driscoll, C.T., 2019. Climate change may alter mercury fluxes in northern hardwood forests. Biogeochemistry 146. https://doi.org/10.5194/acp-16-13399-2016.

Yu, X., Driscoll, C.T., Warby, R.A.F., Montesdeoca, M., Johnson, C.E., 2014. Soil mercury and its response to atmospheric mercury deposition across the northeastern United States. Ecol. Appl. 24, 812–822. https://doi.org/10.1890/13-0212.1.

Zanella, A., Ponge, J., Jabiol, B., Sartori, G., Kolb, E., Gobat, J., Bayon, R.L., Aubert, M., Waal, R.D., Delft, B.V., Vacca, A., Serra, G., Chersich, S., Andreetta, A., Cools, N., Englisch, M., Hager, H., Katzensteiner, K., Brêthes, A., Nicola, C.D., Testi, A., Bernier, N., Graefe, U., Juilleret, J., Banas, D., Garlato, A., Obber, S., Galvan, P., Zampedri, R., Frizzera, L., Tomasi, M., Menardi, R., Fontanella, F., Filoso, C., Dibona, R., Bolzonella, C., Pizzeghello, D., Carletti, P., Langohr, R., Cattaneo, D., Nardi, S., Nicolini, G., Viola, F., 2018. Humusica 1, article 4: terrestrial humus systems and forms — specific terms and diagnostic horizons. Appl. Soil Ecol. 122, 56–74. https://doi.org/10.1016/j.apsoil.2017.07.005.

Zhang, C., Jamieson, R.C., Meng, F., Gordon, R., Bourque, C.P., 2016. Projecting in-stream dissolved organic carbon and total mercury concentrations in small watersheds following forest growth and clearcutting. Water Air Soil Pollut. 227. https://doi.org/10.1007/s11270-016-3017-6.

Zhou, J., Feng, X., Liu, H., Zhang, H., Fu, X., Bao, Z., Wang, X., Zhang, Y., 2013. Examination of total mercury inputs by precipitation and litterfall in a remote upland forest of Southwestern China. Atmos. Environ. 81, 364–372. https://doi.org/10.1016/j.atmosenv.2013.09.010.

Zhou, J., Wang, Z., Zhang, X., Chen, J., 2015. Distribution and elevated soil pools of mercury in an acidic subtropical forest of southwestern China. Environ. Pollut. 202, 187–195. https://doi.org/10.1016/j.envpol.2015.03.021.

Zhou, J., Wang, Z., Zhang, X., Gao, Y., 2017. Mercury concentrations and pools in four adjacent coniferous and deciduous upland forests in Beijing,China. J. Geophys. Res. Biogeosci. 122, 1260–1274. https://doi.org/10.1002/2017JG003776.

Zhou, J., Wang, Z., Zhang, X., 2018. Deposition and fate of mercury in litterfall, litter, and soil in coniferous and broad-leaved forests. J. Geophys. Res. Biogeosci. 123 (8), 2590–2603. https://doi.org/10.1029/2018JG004415.